Dalton Transactions

PAPER

View Article Online
View Journal

Cite this: DOI: 10.1039/c5dt04845a

Synthesis of a rhodium(I) germyl complex: a useful tool for C–H and C–F bond activation reactions†‡

Theresia Ahrens, Mike Ahrens, Thomas Braun,* Beatrice Braun and Roy Herrmann

The dihydrido germyl complex *cis,fac*-[Rh(GePh$_3$)(H)$_2$(PEt$_3$)$_3$] (**2**) was synthesized by an oxidative addition of HGePh$_3$ at [Rh(H)(PEt$_3$)$_3$] (**1**). Treatment of **2** with neohexene generated the rhodium(I) germyl complex [Rh(GePh$_3$)(PEt$_3$)$_3$] (**3**). Alternatively, treatment of the methyl complex [Rh(CH$_3$)(PEt$_3$)$_3$] (**4**) with HGePh$_3$ furnished at room temperature also **3**. Low-temperature NMR measurements revealed an initial formation of the oxidative addition product *fac*-[Rh(GePh$_3$)(H)(CH$_3$)(PEt$_3$)$_3$] (**5**), which transforms into the intermediate complex [Rh(GePh$_3$)(H)(CH$_3$)(PEt$_3$)$_2$] (**6**) by dissociation of a triethylphosphine ligand. The reductive elimination of methane and coordination of PEt$_3$ afforded the germyl complex **3**. Treatment of **3** with CO gave the biscarbonyl complex [Rh(GePh$_3$)(CO)$_2$(PEt$_3$)$_2$] (**7**). The molecular structures of the complexes **2**, **3** and **7** were determined by X-ray crystallography. The germyl complex **3** reacted with 2,3,5,6-tetrafluoropyridine or pentafluorobenzene to furnish the C–H activation products [Rh(4-C$_5$NF$_4$)(PEt$_3$)$_3$] (**8**) and [Rh(C$_6$F$_5$)(PEt$_3$)$_3$] (**9**), respectively. The reaction of **3** with hexafluorobenzene or perfluorotoluene gave selectively the C–F activation products **9** and [Rh(4-C$_6$F$_4$CF$_3$)(PEt$_3$)$_3$] (**10**). Treatment of **3** with pentafluoropyridine resulted in the formation of the C–F activation products **8** and [Rh(2-C$_5$NF$_4$)(PEt$_3$)$_3$] (**11**) in a 1 : 10 ratio. The two isomeric activation compounds [Rh{(*E*)-CF=CF(CF$_3$)}(PEt$_3$)$_3$] (**12**) and [Rh{(*Z*)-CF=CF(CF$_3$)}(PEt$_3$)$_3$] (**13**) were obtained in a 3 : 1 ratio by reaction of **3** with hexafluoropropene. On exposure to oxygen the highly air sensitive complex **12** reacts to yield the peroxido-bridged dirhodium complex [Rh{(*E*)-CF=CF(CF$_3$)}(μ–κ^1:η^2-O$_2$)(PEt$_3$)$_2$]$_2$ (**14**). The molecular structure of **14** was determined by X-ray crystallography.

Received 11th December 2015,
Accepted 2nd February 2016

DOI: 10.1039/c5dt04845a

www.rsc.org/dalton

Introduction

In the past few decades the interest in fluorinated molecules as building blocks has increased drastically due to their applications in agrochemicals, pharmaceuticals and advanced materials.[1–6] The activation of C–F bonds mediated by transition-metal complexes is meanwhile a fairly well established research area.[7–25] The selective C–F bond cleavage in highly fluorinated or perfluorinated molecules can represent a unique way to access fluorinated building blocks. Thus, in the coordination sphere of a metal complex new fluorinated molecules can be formed, which are otherwise not accessible or difficult to access.[7–65] Note that transition-metal mediated fluorination reactions provide an alternative way to synthesize fluorinated compounds.[66–78] The thermodynamic driving force for C–F bond activation reactions at transition-metal centers is usually the formation of another strong bond like a H–F, Si–F, B–F, Al–F or even a M–F bond.[23,79] C–F activation reactions for which a strong germanium–fluorine bond is formed are rare and have not been reported for transition-metal mediated reactions.[80] At rhodium, Milstein *et al.* demonstrated that the rhodium(I) silyl complexes [Rh(SiR$_3$)(PMe$_3$)$_3$] (SiR$_3$ = SiMe$_2$Ph, SiPh$_3$) react with hexafluorobenzene to afford the fluoroaryl complex [Rh(C$_6$F$_5$)(PMe$_3$)$_3$] and the corresponding fluorosilanes.[81] Furthermore, a catalytic conversion of hexafluorobenzene into pentafluorobenzene was achieved by using [Rh(H)(PMe$_3$)$_4$] as catalyst.[82] Later it was shown that [Rh(H)(PEt$_3$)$_3$] (**1**) is also suitable to activate pentafluoropyridine as well as hexafluoropropene by a selective C–F bond cleavage.[83–85] The latter reaction resulted in the formation of the (*Z*)-C–F activation product [Rh{(*Z*)-CF=CF(CF$_3$)}(PEt$_3$)$_3$] (**13**) which catalyses in the presence of hydrosilanes the selective formation of 3,3,3-trifluoropropylsilane from hexafluoropropene.[52]

Herein we report on the synthesis of a unique 16-electron rhodium(I) germyl complex [Rh(GePh$_3$)(PEt$_3$)$_3$] (**3**) and its reactivity towards small molecules like CO and H$_2$. Furthermore, reactivity studies concerning C–H and C–F bond activation reactions of highly fluorinated pyridines, aromatics and hexafluoropropene are described.

Humboldt-Universität zu Berlin, Department of Chemistry, Brook-Taylor-Straße 2, D-12489 Berlin, Germany. E-mail: thomas.braun@chemie.hu-berlin.de

† Dedicated to Prof. Erhard Kemnitz on the occasion of his 65th birthday.

‡ Electronic supplementary information (ESI) available. CCDC 1438402–1438406. For ESI and crystallographic data in CIF or other electronic format see DOI: 10.1039/c5dt04845a

Results and discussion

Treatment of the hydrido complex [Rh(H)(PEt_3)$_3$] (**1**) with $HGePh_3$ led to the formation of the oxidative addition product *cis,fac*-[Rh($GePh_3$)$(H)_2$(PEt_3)$_3$] (**2**) (Scheme 1).

The $^{31}P\{^1H\}$ NMR spectrum of the rhodium(III) complex **2** shows the expected splitting pattern. A doublet of triplets at δ = 15.5 ppm ($^1J_{Rh,P}$ = 100 Hz) for the phosphine ligand in the *trans*-position to the germyl ligand and a doublet of doublets at δ = 11.1 ppm ($^1J_{Rh,P}$ = 96 Hz) for the phosphine ligands in the *trans*-position to the hydrido ligands. The values for the phosphorus–rhodium coupling constants are characteristic for a Rh^{III} species.[86,87] The ^1H NMR spectrum reveals for both hydrido ligands a resonance signal at δ = −11.3 ppm which is of higher order. The coupling constants were determined by simulation of the ^1H NMR spectrum (Fig. 1).[88] The pattern indicates a large phosphorus–hydrogen coupling constant which is typical for a phosphine ligand in the *trans*-position.[52,54,84,89–91] In the $^1H\{^{31}P\}$ decoupling experiment the signal simplified to a doublet due to the coupling to the rhodium atom (Fig. 1, top). The IR spectrum of **2** displays two absorption bands at $\tilde{\nu}$ = 2025 and 1968 cm^{-1} which are assigned to the RhH_2 vibrations and the data are comparable to those of known rhodium dihydrido complexes.[52,84] In addition DFT calculations support also the presence of two absorption bands (see ESI‡). The Rh(I) complex [Rh(acac)-($GeEt_3$)(H)(PCy_3)] ($\tilde{\nu}$ = 2060 cm^{-1}, acac = acetylacetonate) or [Rh(Cl)(H)(GeR_3)(PPh_3)$_2$] (R = Me, Et; $\tilde{\nu}$ = 2107–2035 cm^{-1}) show absorption bands which are shifted towards higher wavenumbers.[92–94] The molecular structure of **2** in the solid state was determined by X-ray crystallography (Fig. 2). Light yellow crystals were obtained from a toluene/*n*-hexane solution at 243 K. Selected bond lengths and angles are summarized in Table 1. Note that the asymmetric unit contains three crystallographically independent molecules which show only minor differences in bond lengths and angles. Therefore, only one will be discussed and is shown as an ORTEP diagram (Fig. 2).

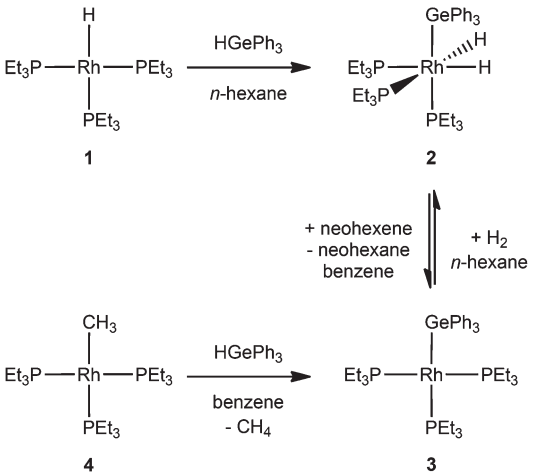

Scheme 1 Synthesis of the rhodium(I) germyl complex [Rh($GePh_3$)-(PEt_3)$_3$] (**3**).

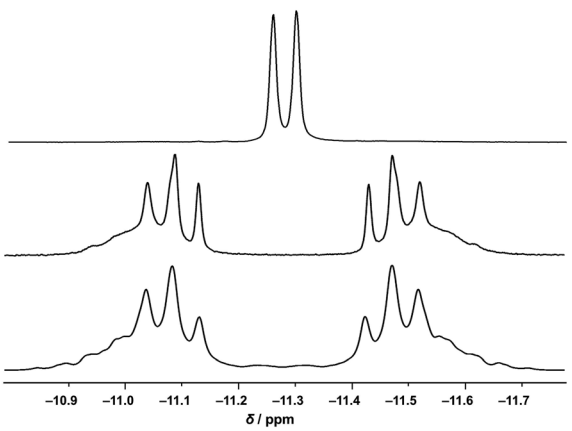

Fig. 1 Part of the ^1H NMR spectrum of complex **2**; simulated (bottom) observed (middle) and part of the $^1H\{^{31}P\}$ NMR spectrum (top) using the following coupling constants (Hz): $^1J(Rh,P^a)$ = $^1J(Rh,P^{a'})$ = 100.6, $^1J(Rh,P^b)$ = 95.7, $^2J(P^a,P^b)$ = $^2J(P^{a'},P^b)$ = 22.1, $^2J(P^a,P^{a'})$ = 20.3,[1] $J(Rh,H^x)$ = $^1J(Rh,H^{x'})$ = 13.7, $^2J(P^a,H^x)$ = $^2J(P^{a'},H^{x'})$ = 133.7, $^2J(P^{a'},H^x)$ = $^2J(P^a,H^{x'})$ = −21.1, $^2J(P^b,H^x)$ = $^2J(P^b,H^{x'})$ = 16.8, $^2J(H^x,H^{x'})$ = 4.8.

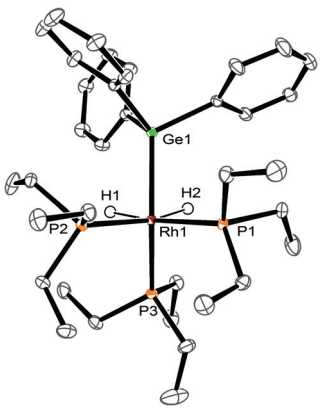

Fig. 2 An ORTEP diagram of **2**. Ellipsoids are drawn at the 50% probability level. C–H hydrogen atoms were omitted for clarity. The rhodium-bound hydrogen atoms were located in the difference Fourier map and refined isotropically.

Table 1 Selected bond lengths [Å] and angles [°] in *cis,fac*-[Rh($GePh_3$)$(H)_2$(PEt_3)$_3$] (**2**)

Lengths [Å]			
P1–Rh1	2.3738(5)	Ge1–Rh1	2.4502(5)
P2–Rh1	2.3718(6)	H1–Rh1	1.56(3)
P3–Rh1	2.3430(5)	H2–Rh1	1.51(3)
Angles [°]			
P1–Rh1–P2	104.393(15)	P3–Rh1–H1	80.1(10)
P1–Rh1–P3	104.013(18)	Ge1–Rh1–H1	76.9(10)
P2–Rh1–P3	104.459(16)	Ge1–Rh1–H2	72.1(9)
P1–Rh1–Ge1	96.338(13)	P1–Rh1–H2	83.8(9)
P2–Rh1–Ge1	97.932(13)	P2–Rh1–H2	168.0(9)
P3–Rh1–Ge1	144.633(13)	P3–Rh1–H2	81.6(9)
P1–Rh1–H1	172.2(10)	H1–Rh1–H2	90.3(14)
P2–Rh1–H1	80.7(10)		

The molecular structure of **2** reveals a distorted octahedral coordination geometry at the metal center where the three phosphine ligands occupy the facial positions. Both metal bound hydrogen atoms were located in the difference Fourier map and refined isotropically. The two hydrido ligands are located in a mutually *cis*-position to each other. The P–Rh–P angles and the Ge–Rh–P angels are all larger than 90° indicating the slight distortion. The rhodium–phosphorus bond length of 2.3430(5) Å in the *trans*-position to the Ge atom is noticeably shorter than the other two rhodium–phosphorus bond lengths [2.3738(5) and 2.3718(6) Å]. When compared to the corresponding distances found in the structural related silyl complexes *cis*,*fac*-[Rh(H)$_2$(SiClPh$_2$)(PMe$_3$)$_3$] [Rh–P *trans* to Si = 2.334(2) Å], *cis*,*fac*-[Rh(H)$_2$\{SiPh$_2$(SPh)\}(PMe$_3$)$_3$] [Rh–P *trans* to Si = 2.336(1) Å] and *cis*,*fac*-[Rh(H)$_2$\{Si(C$_6$H$_4$CF$_3$)$_3$\}(PMe$_3$)$_3$] [Rh–P *trans* to Si = 2.326(4) Å], The Rh–P bond length is in a similar range which might imply a comparable *trans* influence of the germyl ligand as the silyl ligand.[84,95–97] The Rh(1)–Ge(1) bond length of 2.4502(5) Å is shorter than the distance in carbonyl complexes like [Rh(GePh$_3$)(CO)$_4$] [Rh–Ge = 2.5061(4) Å].[98]

The reaction of [Rh(GePh$_3$)(H)$_2$(PEt$_3$)$_3$] (**2**) with neohexene resulted in the formation of the 16 electron rhodium(I) germyl complex [Rh(GePh$_3$)(PEt$_3$)$_3$] (**3**, Scheme 1). Note that the oxidative addition of H$_2$ at **3** affords again the dihydrido complex **2**. The ^{31}P\{^{1}H\} NMR spectrum of **3** depicts a doublet of doublets at δ = 11.1 ppm ($^1J_{Rh,P}$ = 143, $^2J_{P,P}$ = 36 Hz) for the phosphine ligand in a mutually *trans*-position and a doublet of triplets at δ = 6.5 ppm ($^1J_{Rh,P}$ = 136, $^2J_{P,P}$ = 36 Hz). The rhodium–phosphorus coupling constants indicate the presence of a Rh(I) species.[56,91,99–101] The molecular structure of **3** in the solid state was determined by X-ray crystallography (Fig. 3). Selected bond lengths and angles are summarized in Table 2. Suitable crystals of **3** were grown from a saturated *n*-hexane solution at 243 K. The structure exhibits a distorted square-planar coordination geometry at the metal center. The Rh(1)–Ge(1) distance [2.46459(18) Å] is in a similar range to those found for complex **2**. The Rh–P distances [2.2822(4)–2.3268(4) Å] are – when compared to **2** – shorter, but in the same range like these in the structural related silyl complexes [Rh(SiPh$_3$)(PMe$_3$)$_3$] and [Rh(SiMe$_2$Ph)(PMe$_3$)$_3$] [2.266(1)–2.332(1) Å].[89,90] The formation of **3** from [Rh(CH$_3$)(PEt$_3$)$_3$] (**4**) and HGePh$_3$ was also monitored by low temperature NMR spectroscopy. The studies reveal the initial generation of the oxidative addition product *fac*-[Rh(GePh$_3$)(H)(CH$_3$)(PEt$_3$)$_3$] (**5**) at 203 K (Scheme 2). The latter converts into [Rh(GePh$_3$)(H)(CH$_3$)(PEt$_3$)$_2$] (**6**) at 213 K by phosphine dissociation. The reductive elimination of methane affords the 16 electron rhodium(I) germyl complex [Rh(GePh$_3$)(PEt$_3$)$_3$] (**3**). The reaction is inhibited by free phosphine indicating that the reductive elimination of methane does not occur from **5**, but from complex **6**.

The ^{31}P\{^{1}H\} NMR spectrum of **5** displays three doublets of triplets at δ = 13.1, 9.4 and 5.7 ppm (Fig. 4).[102] The rhodium–phosphorus coupling constants ($^1J_{Rh,P}$ = 93–87 Hz) and the phosphorus–phosphorus coupling constants ($^2J_{P,P} \approx$ 22 Hz) are compatible with the assignment as a Rh^{III} complex.[86,87] The observed pattern is in accordance with a *fac*-configuration for **5**. The ^{1}H NMR spectrum of **5** shows a broad signal at δ = 0.16 ppm which can be assigned to the methyl group. The resonance signal for the hydrido ligand appears as a doublet of doublets of triplets at δ = −10.69 ppm ($^2J_{H,P\text{-}cis}$ = 20 Hz, $^1J_{H,Rh} \approx {}^2J_{H,P\text{-}cis} \approx$ 11 Hz) revealing a large phosphorus–hydrogen coupling of 157 Hz to a phosphine ligand at the *trans*-position (Fig. 5). In a ^{31}P decoupling experiment the signal simplified to a doublet confirming the $^1J_{H,Rh}$ coupling constant. An additional ^{1}H,^{31}P HMBC NMR spectrum, which was optimized to a large H,P coupling constant, reveals a correlation peak for

Table 2 Selected bond lengths [Å] and angles [°] in [Rh(GePh$_3$)(PEt$_3$)$_3$] (**3**)

Lengths [Å]			
P1–Rh1	2.2822(4)	P3–Rh1	2.3268(4)
P2–Rh1	2.3162(4)	Ge1–Rh1	2.46459(18)
Angles [°]			
P1–Rh1–P2	95.987(13)	P1–Rh1–Ge1	91.634(10)
P1–Rh1–P3	149.509(14)	P2–Rh1–Ge1	154.276(11)
P2–Rh1–P3	93.191(13)	P3–Rh1–Ge1	92.558(10)

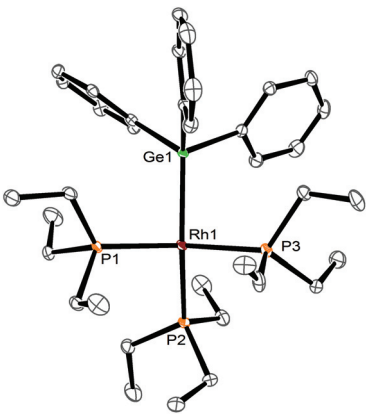

Fig. 3 An ORTEP diagram of **3**. Ellipsoids are drawn at the 50% probability level. C–H hydrogen atoms were omitted for clarity.

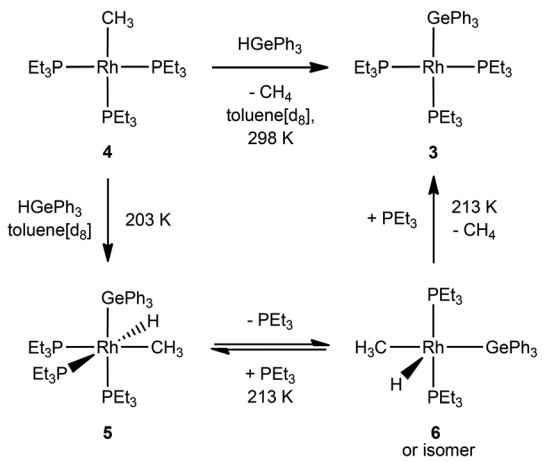

Scheme 2 Reaction pathway for the formation of [Rh(GePh$_3$)(PEt$_3$)$_3$] (**3**).

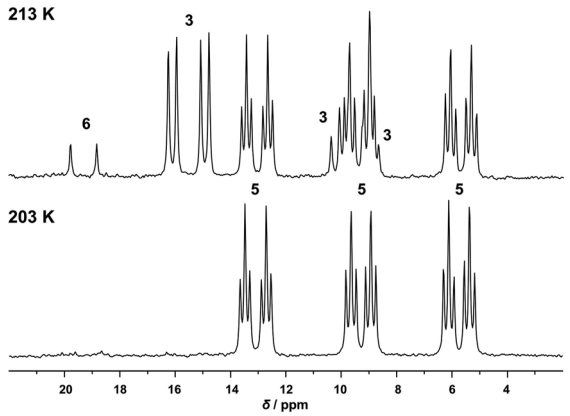

Fig. 4 Part of the $^{31}P\{^{1}H\}$ NMR spectrum of the reaction solution after treatment of **4** with $HGePh_3$ at 203 K (below) and 213 K (above).

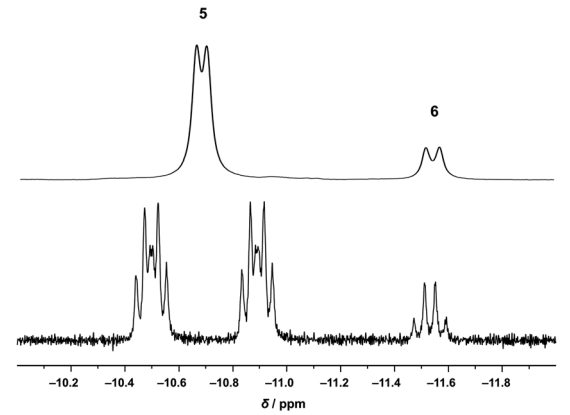

Fig. 5 Part of the ^{1}H NMR spectrum (below, 300 MHz) and part of the $^{1}H\{^{31}P\}$ NMR spectrum (above, 400 MHz) of **5** and **6** at 213 K.

the hydrido ligand and the phosphine ligands in a mutually *trans*-position at $\delta_{H/P}$ = −10/13 ppm which appears as a doublet ($^{2}J_{H,P\text{-}trans}$ = 157 Hz) in the ^{1}H domain. By warming the reaction solution up to 213 K the $^{31}P\{^{1}H\}$ NMR spectrum reveals an additional doublet at δ = 19.3 ppm with a rhodium–phosphorus coupling constant of 115 Hz which can be assigned to the intermediate rhodium complex $[Rh(GePh_3)(H)(CH_3)(PEt_3)_2]$ (**6**). A resonance for the formation of free phosphine was also observed. The ^{1}H NMR spectrum of **6** shows a singlet at δ = 0.26 ppm for the methyl group. Furthermore a second signal at δ = −11.53 ppm appears which simplifies to a doublet ($^{1}J_{H,Rh}$ = 15 Hz) on ^{31}P decoupling and can be assigned to the hydrido ligand. Again a $^{1}H,^{31}P$ HMBC NMR spectrum which was optimized on a small phosphorus–hydrogen coupling constant confirms the structure of **6** by showing a cross peak at $\delta_{H/P}$ = −11/19 ppm. No large hydrido–phosphorus coupling was observed indicating a *cis*-arrangement of both phosphine ligands to the hydrido ligand. To get more information on the structure of **6**, DFT calculations were run on conceivable isomers and the optimized geometry with the lowest energy (**6a**) is depicted in Fig. 6 (see also ESI‡). It was

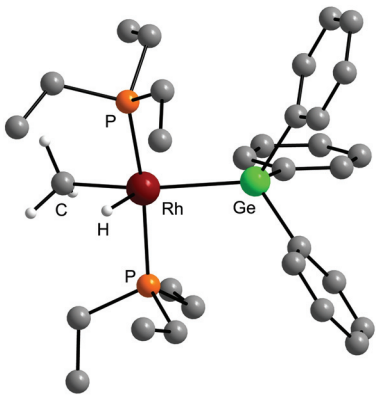

Fig. 6 DFT-optimized structure with the lowest energy of $Rh(GePh_3)(H)(CH_3)(PEt_3)_2]$ (**6**). The hydrogen atoms at the aromatic rings and phosphine ligands are omitted for clarity.

found that the energy differences in the gas phase are small and four minima converged at close energy. Their geometry differs in the ligand that occupies the apical position (H ligand or CH_3 ligand) as well as in the orientation of the ethyl groups at the phosphine ligands. However, the computed structure with the lowest energy shows a distorted square pyramidal coordination arrangement (τ = 0.14)[103] at the central metal atom with the hydrido ligand in the apical position and both phosphine ligands in a mutually *trans*-position. The optimized geometry is in good accordance with the obtained NMR data as well as a presumable *syn* elimination of methane.

Treatment of **3** with CO afforded the biscarbonyl complex $[Rh(GePh_3)(CO)_2(PEt_3)_2]$ (**7**) by replacement of one phosphine ligand (Scheme 3). The $^{31}P\{^{1}H\}$ NMR spectrum for **7** shows at δ = 13.7 ppm a doublet ($^{1}J_{Rh,P}$ = 111 Hz) for both phosphine ligands. Due to a fluxional behavior of **7** in solution only one signal was observed, which did not split into two resonances at low temperature (203 K). A doublet of triplets ($^{1}J_{Rh,C}$ = 65, $^{2}J_{C,P}$ = 1 Hz) in the ^{13}C NMR spectrum at δ = 201.3 ppm can be attributed to the CO ligands. The values for the rhodium–carbon and rhodium–phosphorus coupling constants are in a typical range for rhodium carbonyl complexes bearing two phosphine ligands.[85,90,104] The IR spectrum of **7** exhibits two absorption bands at $\tilde{\nu}$ = 1964 and 1912 cm^{-1} which can be assigned to the $Rh(CO)_2$ unit. The structural related germyl complex $[Rh(GeEt_3)(CO)_2(PPh_3)_2]$ or silyl complex $[Rh\{Si(OEt)_3\}(CO)_2(PMe_3)_2]$ show similar values.[90,93,94]

Suitable crystals for an X-ray diffraction analysis of **7** were obtained from a saturated toluene/*n*-hexane solution at 243 K.

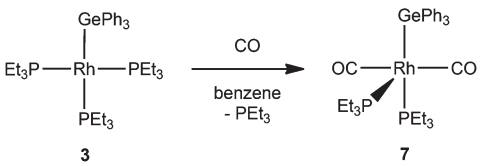

3 **7**

Scheme 3 Formation of the rhodium(I) biscarbonyl complex **7**.

Table 3 Selected bond lengths [Å] and angles [°] in [Rh(GePh$_3$)(CO)$_2$(PEt$_3$)$_2$] (**7**)

Lengths [Å]			
Rh1–P1	2.3448(4)	Rh1–C31	1.8841(15)
Rh1–P2	2.4123(4)	O1–C31	1.1478(19)
Rh1–Ge1	2.4840(19)	O2–C32	1.1476(19)
Rh1–C32	1.8817(15)		
Angles [°]			
P1–Rh1–P2	103.082(14)	C31–Rh1–P1	89.11(5)
P1–Rh1–Ge1	160.307(11)	C32–Rh1–P2	111.17(5)
P2–Rh1–Ge1	96.587(11)	C31–Rh1–P2	113.10(5)
C32–Rh1–C3	134.95(7)	Rh1–C31–O1	175.49(14)
C32–Rh1–P1	88.88(5)	Rh1–C32–O2	175.94(15)

Selected bond lengths and angles are summarized in Table 3. The coordination geometry of the molecular structure of **7** can be considered as either distorted square pyramidal or a distorted trigonal bipyramidal coordination arrangement at the central metal atom (Fig. 7). The parameter τ for complex **7** (0.42) indicates that a description as a square pyramidal structure is more appropriate, for which the phosphine ligand in the *cis*-position to the germyl ligand occupies the apical position.[103] The Rh–P bond lengths [2.3448(4) Å; 2.4123(4) Å] and the Rh–C bond lengths with [1.8817(15) Å; 1.8841(15) Å] are in a typical range. Both rhodium carbonyl units are not linear with a Rh–C–O angle of 175.49(14) and 175.94(15)°. The Rh(1)–Ge(1) distance of 2.4840(19) Å is comparable to these found for the complexes **2** and **3**.

C–H and C–F bond activation reactions

Reactivity studies of the germyl complex [Rh(GePh$_3$)(PEt$_3$)$_3$] (**3**) towards fluorinated pyridines and aromatics as substrates might be of interest concerning C–F and C–H bond activation reactions.[23,25] The treatment of **3** with pentafluorobenzene or 2,3,5,6-tetrafluoropyridine afforded the C–H activation products [Rh(4-C$_5$NF$_4$)(PEt$_3$)$_3$] (**8**) and [Rh(C$_6$F$_5$)(PEt$_3$)$_3$] (**9**), respectively, as well as HGePh$_3$ (Scheme 4). There is no evidence for a C–F bond cleavage. Note that similar C–H bond activations were observed on treatment of the hydrido complex

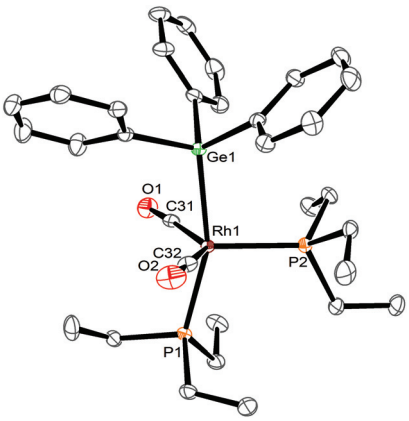

Fig. 7 An ORTEP diagram of **7**. Ellipsoids are drawn at the 50% probability level. C–H hydrogen atoms were omitted for clarity.

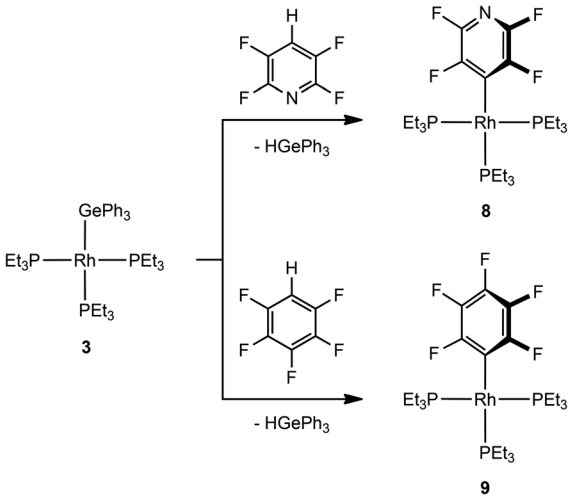

Scheme 4 C–H activation of 2,3,5,6-tetrafluoropyridine and pentafluorobenzene at [Rh(GePh$_3$)(PEt$_3$)$_3$] (**3**).

[Rh(H)(PEt$_3$)$_3$] (**1**) or the boryl complex [Rh(Bpin)(PEt$_3$)$_3$] (pin = pinacolato) with 2,3,5,6-tetrafluoropyridine to give also **8**.[56,85] Marder and Perutz reported that the rhodium silyl complex [Rh(SiPh$_3$)(PMe$_3$)$_3$] is capable of both C–F (2-position) and C–H (4-position) bond activation.[51] It was also reported that the silyl complexes [Rh{Si(OR)$_3$}(PEt$_3$)$_3$] (R = Me, Et) react by C–F bond activation.[91,105]

Complex **3** also reacted with an excess of hexafluorobenzene at 323 K to yield the C–F activation product **9** (Scheme 5). The reaction of **3** with perfluorotoluene at 323 K afforded [Rh(4-C$_6$F$_4$CF$_3$)(PEt$_3$)$_3$] (**10**) with the CF$_3$ group at the *para*-position. Additional free phosphine does not lead to a decrease of the reaction rate indicating that an initial phosphine dissociation does not play a role prior to the C–F activation step. Treatment of **3** with pentafluoropyridine resulted in a C–F bond activation at the 2- and 4-position to yield the activation products [Rh(4-C$_5$NF$_4$)(PEt$_3$)$_3$] (**8**) and [Rh(2-C$_5$NF$_4$)(PEt$_3$)$_3$] (**11**) in a 1 : 10 ratio. The activation at the 2-position may occur by a concerted oxidative addition process.[106–111] An alternative pathway involves a ligand-assisted C–F activation step.[19,20,23,54,56,65,91,112–116] The highly reactive rhodium boryl complex [Rh(Bpin)(PEt$_3$)$_3$] and the silyl complex [Rh{Si(OR)$_3$}(PEt$_3$)$_3$] (R = Me, Et) also furnished the C–F activation products **8**, **9**, **10** and **11** by treatment with the fluorinated pyridine or the aromatic compounds.[56,91,117] The mechanisms for the activation at the 4-position that are commonly discussed in the literature are often linked to a radical pathway or an initial nucleophilic attack of the metal center.[10,118–120] Note that Roesky and Stalke reported on the C–F activation of pentafluoropyridine at the 4-position at the germylene LGeNiPr$_2$ [L = PhC(N*t*Bu)$_2$], but in contrast this conversion proceeds *via* an oxidative addition.[80] Treatment of the germyl complex [Rh(GePh$_3$)(PEt$_3$)$_3$] (**3**) with hexafluoropropene in *n*-hexane led to the formation of the C–F activation product [Rh{(*E*)-CF=CF(CF$_3$)}(PEt$_3$)$_3$] (**12**) and the isomeric complex [Rh{(*Z*)-CF=CF(CF$_3$)}(PEt$_3$)$_3$] (**13**) in a 3 : 1 ratio as well as of FGePh$_3$ after 8 h (Scheme 6). The ratio and

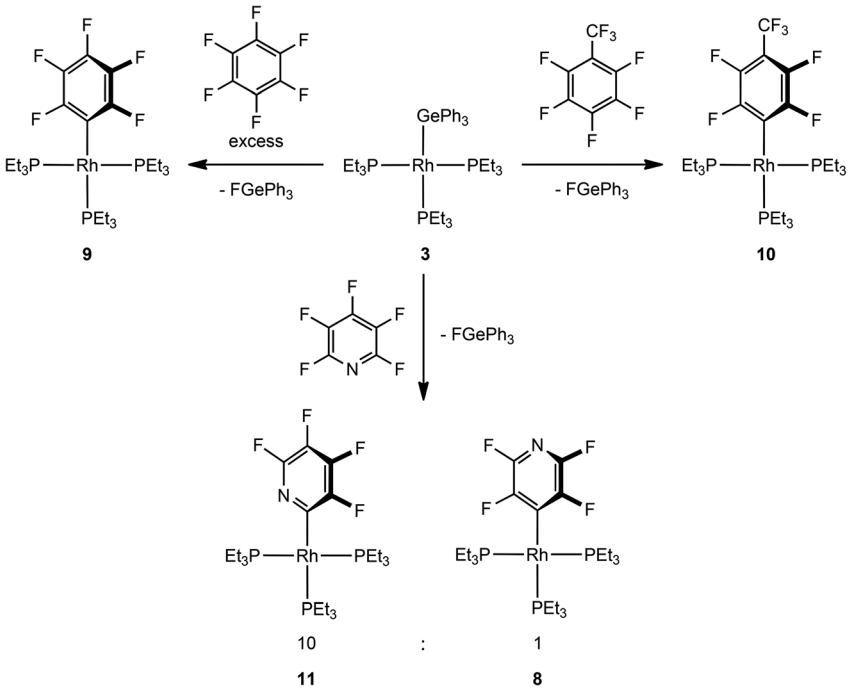

Scheme 5 C–F activation of fluorinated aromatics and pentafluoropyridine at $[Rh(GePh_3)(PEt_3)_3]$.

reaction time are solvent dependent. If the reaction is carried out in benzene a full conversion was achieved after 2 h with a ratio of 12 : 1 for **12** to **13**. The formation of complex **13** has been described before.[83,84] Thus, the hydrido complex $[Rh(H)(PEt_3)_3]$ (**1**) reacts with hexafluoropropene in the presence of Et_3N and Cs_2CO_3 to yield **13**. The $^{31}P\{^1H\}$ and ^{19}F NMR spectra of **12** are of higher order. Therefore the $^{31}P\{^1H\}$ NMR spectrum was computed in order to determine the coupling constants, and the result is depicted in Fig. 8.[88] The ^{19}F NMR spectrum reveals three resonances at δ = −64.4 (CF_3), −78.1 (F^{α}) and −148.0 (F^{β}) ppm in a 3 : 1 : 1 ratio that can be assigned to the propenyl ligand. In contrast to **13** no large fluorine–fluorine coupling constant was observed, which indicates a *cis*-arrangement of the olefinic fluorine atoms.[121] The $^{19}F,^{13}C\{^1H\}$ HMBC NMR spectrum reveals cross-peaks at $\delta_{F/C}$ = −64/123 (CF_3), −78/190 (F^{α}–C^{α}) and −148/140 (F^{β}–C^{β}) ppm which supports the structural assignment for **12**.[84] The reaction of an *in situ* generated mixture of **12** and **13** with dioxygen led to the instant formation of a dinuclear peroxido-bridged rhodium complex $[Rh\{(E)\text{-}CF{=}CF(CF_3)\}(\mu\text{-}\kappa^1{:}\eta^2\text{-}O_2)(PEt_3)_2]_2$ (**14**), which exhibits a rare coordination mode of the O_2 units (Scheme 7), as well as $OPEt_3$. The formation of the isomeric compound $[Rh\{(Z)\text{-}CF{=}CF(CF_3)\}(\mu\text{-}\kappa^1{:}\eta^2\text{-}O_2)(PEt_3)_2]_2$ was not observed presumably due to decomposition reactions.

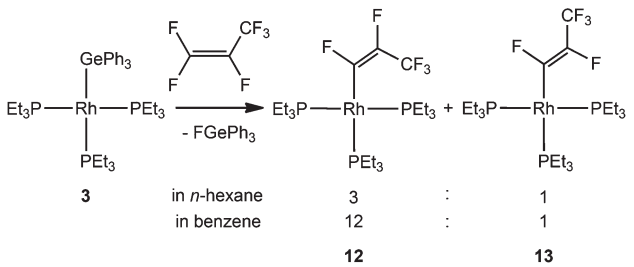

Scheme 6 C–F activation of hexafluoropropene at the rhodium(I) germyl complex **3**.

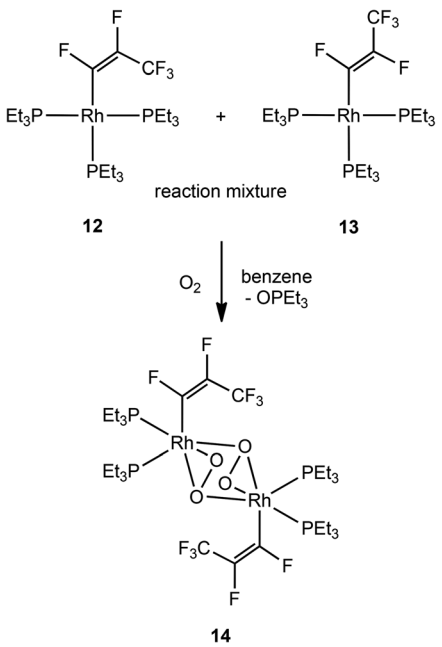

Scheme 7 Selective oxygenation reaction of the C–F activation product **12**.

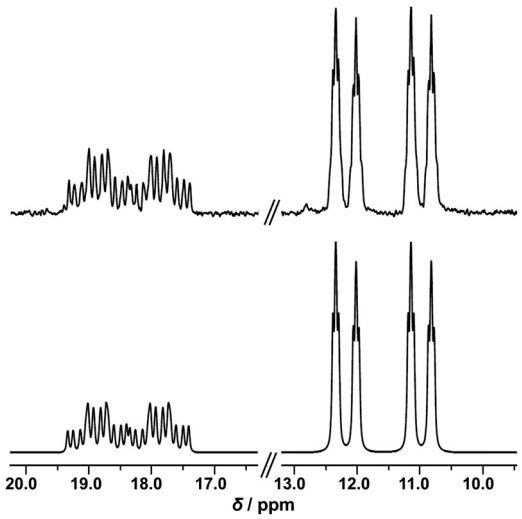

Fig. 8 Part of the $^{31}P\{^1H\}$ NMR spectrum of complex **12**; simulated (below) observed (above) using the following coupling constants (Hz): $^1J(Rh,P^a)$ = 145.3, $^1J(Rh,P^b)$ = 120.3 $^2J(P^a,P^b)$ = 39.3, $^3J(P^a,F^\alpha)$ = 4.7, $^4J(P^a,F^\beta)$ = 6.7, $^5J(P^a,F)$ = 0.8, $^3J(P^b,F^\alpha)$ = 24.4, $^4J(P^b,F^\beta)$ = 10.6, $^5J(P^b,F)$ = 1.5.

Note that in comparable reactions usually the formation of mononuclear peroxido complexes was observed.[99,100,122,123] The $^{31}P\{^1H\}$ NMR spectrum of **14** shows a doublet of doublets at δ = 26.4 ppm due to the coupling to the rhodium atom ($^1J_{Rh,P}$ = 121 Hz) and to the fluorine atom ($^3J_{P,F}$ = 29 Hz) at the α-carbon atom of the pentafluoropropenyl ligand. The rhodium-phosphorus coupling constant is in a typical range for a binuclear Rh(III) spezies.[124–127] The ^{19}F NMR spectrum depicts three resonances at δ = −65.5 (CF_3), −66.5 (F^α) and −143.6 (F^β) ppm in a 6 : 2 : 2 ratio for the propenyl ligand. The chemical shifts are in a similar range than those found for **12** or **13**.[83,84] Two polymorphic structures of **14** (**14a** and **14b**) in the solid state were determined by X-ray crystallography (Fig. 9 for **14a** and ESI‡ for **14b**). Due to the structural similarities only the data for **14a** are discussed in the following. Yellow

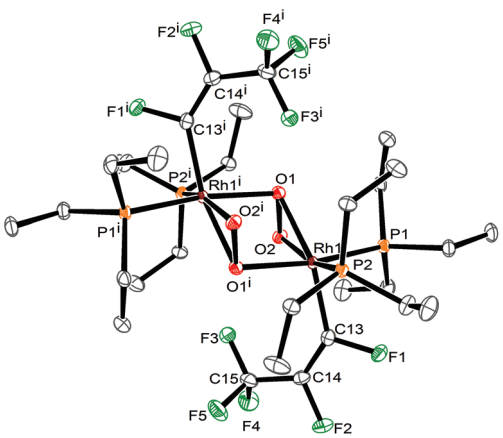

Fig. 9 An ORTEP diagram of **14a**. Ellipsoids are drawn at the 50% probability level. C–H hydrogen atoms were omitted for clarity.

Table 4 Selected distances [Å] and angles [°] in [Rh{(*E*)-CF=CF(CF_3)}(μ–κ^1:η^2-O_2)(PEt_3)$_2$]$_2$ (**14a**)

Lengths [Å]			
Rh1–O1	2.1542(12)	O2–O2^i	3.5561(17)
Rh1^i–O1	2.0954(12)	O1–O2^i	2.7737(18)
Rh1–O2	1.9988(13)	C13–C14	1.331(3)
Rh1–P1	2.2900(5)	C13–F1	1.400(2)
Rh1–P2	2.3411(5)	C14–F2	1.372(2)
Rh1–C13	1.9999(19)	Rh1–O_{middle}	1.9436(13)
O1–O2	1.4702(17)	Rh1^i–O_{middle}	2.3598(13)
O1–O1^i	2.6578(18)		
Angles [°]			
O1–Rh1–P1	90.15(3)	O2–O1–Rh1	63.70(7)
O1–Rh1–P2	119.91(4)	O2^i–O1^i–Rh1	101.94(8)
O2–Rh1–P1	81.20(4)	O2–Rh1–C13	109.93(6)
O2–Rh1–P2	160.71(4)	C13–Rh1–O1	150.90(6)
P2–Rh1–P1	106.315(18)	C13–Rh1–O1^i	99.79(6)
O2–Rh1–O1	41.25(5)	C13–Rh1–P1	87.99(5)
O1–Rh1–O1^i	77.42(5)	C13–Rh1–P2	88.36(5)
O2–Rh1–O1^i	85.26(5)	Rh1–O1–Rh1^i	102.58(5)
O1^i–Rh1–P1	166.07(4)	O1–O2–Rh1	75.05(7)
O1^i–Rh1–P2	85.59(4)		

crystals (block) of **14a** were obtained from a toluene/*n*-hexane solution at 243 K. Selected bond lengths and angles are summarized in Table 4. In the solid state complex [Rh{(*E*)-CF=CF(CF_3)}(μ–κ^1:η^2-O_2)(PEt_3)$_2$]$_2$ (**14a**) adopts a binuclear coordination mode in which two peroxido ligands bridge two rhodium centers *via* one oxygen atom of the peroxido units. The geometry around the rhodium centers can be either described as approximately trigonal-bipyramidal, if the peroxido unit is treated as occupying a single coordination site or as a distorted octahedral structure if it is regarded as a bidentate ligand. The latter seems to be more appropriate and is consistent with the oxidation state III at the rhodium center which was suggested by the obtained NMR data. The Rh(1)–O(1) and Rh(1)–O(2) bond lengths with 2.1542 (12) Å and 1.9988(13) Å differ noticeably from each other resulting in an asymmetrical bridging whereas the oxygen atom with the longer Rh–O bond length exhibits a shorter distance to the other metal center [Rh(1^i)–O(1) = 2.0954(12) Å]. The O(1)–O(2) separation of 1.4702(17) Å is consistent with the distances found for other rhodium η^2-peroxido complexes.[99,100,122,128–133] The values for the Rh–C, C=C as well as the C–F bond lengths of the pentafluoropropenyl ligand are comparable to these found for complex **13**.[83] For late transition-metal complexes the rhodium complexes [Rh(μ–κ^1:η^2-O_2)($PhBP_3$)]$_2$ [$PhBP_3$ = tris(methylenediphenylphosphane)phenylborate] and [Rh(Cl)(μ–κ^1:η^2-O_2)(PPh_3)$_2$]$_2$ as well as the palladium complex [{Pd(κ^2-Tp^{iPr})}$_2$(μ–κ^1:η^2-O_2)(py)] [Tp^{iPr} = hydridotris(3,5-diisopropylpyrazolyl)-borato] are the only three precedents reported in the literature which exhibit such an unusual μ–κ^1:η^2-O_2-bridging mode.[134–137]

Conclusions

In this paper we report on the synthesis of the 16 electron rhodium(I) germyl complex [Rh($GePh_3$)(PEt_3)$_3$] (**3**) and its reactivity towards highly fluorinated substrates. The studies

revealed that the germyl complex **3** is a useful tool for C–F bond activation reactions which extend the range of suitable rhodium(I) complexes in this field. It was found that the formation of **3**, reacting $[Rh(CH_3)(PEt_3)_3]$ (**3**) with $HGePh_3$, was initiated *via* a PEt_3 dissociation at *fac*-$[Rh(GePh_3)(H)(CH_3)(PEt_3)_3]$ (**5**) and recoordination. For the preferred formation of the C–F activation product $[Rh(2\text{-}C_5NF_4)(PEt_3)_3]$ (**11**) a ligand-assisted process is conceivable, which involves an interaction of the germyl ligand with a fluorine atom. This conversion extends the range of C–F activation reactions at rhodium(I) complexes such as $[Rh(H)(PEt_3)_3]$, $[Rh(Bpin)(PEt_3)_3]$, $[Rh(Bcat)(PEt_3)_3]$, $[Rh(SiPh_3)(PMe_3)_3]$ or $[Rh\{Si(OEt)_3\}(PEt_3)_3]$.[56,81,85,91,117] The treatment of the germyl complex **3** with hexafluoropropene led to a new C–F activation product $[Rh\{(E)\text{-}CF{=}CF(CF_3)\}(PEt_3)_3]$ (**12**) as a major product. Exposure of **12** to an oxygen atmosphere gave the dinuclear peroxido-bridged rhodium complex $[Rh\{(E)\text{-}CF{=}CF(CF_3)(\mu\text{-}\kappa^1{:}\eta^2\text{-}O_2)(PEt_3)_2\}_2$ (**14**) which exhibits a rare coordination mode of the O_2 moiety.

Experimental

General methods and instrumentations

The synthetic work was carried out with a Schlenk line or in a glove box under an atmosphere of argon. All solvents were purified and dried by conventional methods and distilled under an atmosphere of argon before use. $[D_6]$Benzene, $[D_8]$thf and $[D_8]$toluene were dried by stirring over Na/K and then distilled. Triphenylgermane was obtained from ABCR and used without further purification. $[Rh(H)(PEt_3)_3]$ (**1**) and $[Rh(CH_3)(PEt_3)_3]$ (**4**) were prepared according to the literature.[87,138,139] The NMR spectra were acquired on a Bruker DPX 300, Bruker Avance 300 or Bruker Avance 400 spectrometer. The ^{1}H and ^{13}C NMR chemical shifts were referenced to residual $[D_5]$benzene at δ = 7.15 ppm, $[D_7]$thf at δ = 1.73 ppm or $[D_7]$toluene at δ = 2.09 ppm. The ^{19}F NMR spectra were referenced to external $CFCl_3$ at δ = 0.0 ppm. The $^{31}P\{^1H\}$ NMR spectra were referenced externally to 85% H_3PO_4 at δ = 0.0 ppm. Infrared spectra were recorded on a Bruker Vertex 70 spectrometer that was equipped with an ATR unit (diamond). Mass spectrometry was measured with a Micromass Q-TOF-2 mass spectrometer which was equipped with a Linden LIFDI source (Linden CMS GmbH). Microanalyses were performed with a HEKAtech Euro EA 3000 elemental analyzer.

Synthesis of $[Rh(GePh_3)(H)_2(PEt_3)_3]$ (2). (a) A solution of $HGePh_3$ (113 mg, 0.37 mmol) in *n*-hexane (2 mL) was added to a solution of $[Rh(H)(PEt_3)_3]$ (**1**) (170 mg, 0.37 mmol) in *n*-hexane (4 mL). The reaction mixture turned from dark red to pale yellow within seconds. After stirring for 30 min the reaction mixture was filtered. The residue was washed twice with *n*-hexane (3 mL) and dried *in vacuo* to obtain **2** as a pale yellow solid. Yield 257 mg (89%).

(b) A slow stream of hydrogen was bubbled through a solution of $[Rh(GePh_3)(PEt_3)_3]$ (**3**) (153 mg, 0.20 mmol) in *n*-hexane (5 mL) for 2 min at room temperature. The solution turned from dark red to yellow. After stirring for 30 min a pale yellow solid precipitated. The solvent was filtered of and the residue was dried *in vacuo* to obtain **2** as a pale yellow solid. Yield 137 mg (90%). Analytical data for **2**: $C_{36}H_{62}GeP_3Rh$ (764.34): calcd C, 56.64; H, 8.19; found: C, 56.87; H, 8.21. **IR** (ATR) $\tilde{\nu}$ (cm^{-1}): 2025, 1968 (RhH_2). **^{1}H NMR** (500.1 MHz, $[D_8]$thf): δ = 7.59 (m, dd in the $^1H\{^{31}P\}$ NMR spectrum, ^3J(H,H) = 8, ^4J(H,H) = 2 Hz, 6H; Ph), 7.07–6.99 (m, 9H; Ph), 1.80 (m, q in the $^1H\{^{31}P\}$ NMR spectrum ^3J(H,H) = 8 Hz, 6H; PCH_2CH_3), 1.50 (m, q in the $^1H\{^{31}P\}$ NMR spectrum ^3J(H,H) = 8 Hz, 12H; PCH_2CH_3), 1.17 (dt, ^3J(H,P) = 13, ^3J(H,H) = 8 Hz, 9H; PCH_2CH_3), 0.87 (dt, ^3J(H,P) = 14, ^3J(H,H) = 8 Hz, 18H; PCH_2CH_3), −11.28 (m, ^1J(Rh,P^a) = ^1J(Rh,$P^{a'}$) = 100.6, ^1J(Rh,P^b) = 95.7, ^2J(P^a,P^b) = ^2J($P^{a'}$,P^b) = 22.1, ^2J(P^a,$P^{a'}$) = 20.3, ^1J(Rh,H^x) = ^1J(Rh,$H^{x'}$) = 13.7, ^2J(P^a,H^x) = ^2J($P^{a'}$,$H^{x'}$) = 133.7, ^2J($P^{a'}$,H^x) = ^2J(P^a,$H^{x'}$) = −21.1, ^2J(P^b,H^x) = ^2J(P^b,$H^{x'}$) = 16.8, ^2J(H^x,$H^{x'}$) = 4.8 Hz, 2H; RhH) ppm. The coupling constants were determined by simulation with gNMR.[88] **$^{31}P\{^1H\}$ NMR** (121.5 MHz, $[D_6]$benzene): δ = 15.5 (dt, ^1J(Rh,P) = 100, ^2J(P,P) = 20 Hz, 1P), 11.1 (dd, ^1J(Rh,P) = 96, ^2J(P,P) = 20 Hz, 2P) ppm. **MS** (LIFDI, toluene), *m*/*z*: 764 $[M]^+$.

Synthesis of $[Rh(GePh_3)(PEt_3)_3]$ (3). (a) A solution of $[Rh(GePh_3)(H)_2(PEt_3)_3]$ (**2**) (118 mg, 0.15 mmol) in benzene (2 mL) was treated with neohexene (50 μL, 0.38 mmol). The reaction mixture was stirred for 2 h at room temperature. All volatiles were removed *in vacuo* and a dark red solid remained. Yield 113 mg (99%).

(b) A solution of $[Rh(CH_3)(PEt_3)_3]$ (**3**) (153 mg, 0.32 mmol) in *n*-hexane (4 mL) was treated with a solution of $HGePh_3$ (98 mg, 0.32 mmol) in *n*-hexane (1 mL). The reaction mixture was stirred for 30 min at room temperature. All volatiles were removed *in vacuo*. A dark red solid was obtained. Yield 242 mg (98%). Analytical data for **3**: $C_{36}H_{60}P_3GeRh$ (761.32): calcd C, 56.79; H, 7.94; found: C, 56.68; H, 7.95. **^{1}H NMR** (300.1 MHz, $[D_6]$benzene): δ = 8.10 (m, 6H; Ph), 7.20 (m, 6H; Ph), 7.18 (m, 3H; Ph), 1.66–1.40 (m, 18H; PCH_2CH_3), 1.20–0.76 (m, 27H; PCH_2CH_3) ppm. **$^{31}P\{^1H\}$ NMR** (121.5 MHz, $[D_6]$benzene) δ = 11.1 (dd, ^1J(Rh,P) = 143, ^2J(P,P) = 36 Hz, 2P), 6.5 (dt, ^1J(Rh,P) = 136, ^2J(P,P) = 36 Hz, 1P) ppm. **MS** (LIFDI, toluene), *m*/*z*: 762 $[M]^+$.

Formation of *fac*-$[Rh(GePh_3)(H)(CH_3)(PEt_3)_3]$ (5). A solution of $HGePh_3$ (20 mg, 65 μmol) in $[D_8]$toluene (0.1 mL) was added to a solution of $[Rh(CH_3)(PEt_3)_3]$ (**4**) (31 mg, 65 μmol) in $[D_8]$toluene (0.4 mL) at 183 K. The NMR spectroscopic data of the reaction solution at 203 K revealed a complete conversion of **4** into **5**. Analytical data for **5**: **^{1}H NMR** (300.1 MHz, $[D_8]$-toluene, 203 K) δ = 8.19 (d, ^3J(H,H) = 7 Hz, 6H, Ph), 7.32 (m, 6H; Ph), 7.22 (m 3H;Ph), 1.63 (m, 6H; PCH_2CH_3), 1.47 (m, 9H; PCH_2CH_3), 1.00–0.60 (m, 30H; PCH_2CH_3), 0.16 (br s, 3H; CH_3), −10.69 (ddt, d in the $^1H\{^{31}P\}$ NMR spectrum, ^2J(H,P_{trans}) = 157, ^2J(H,P_{cis}) = 20, ^1J(H,Rh) = 11, ^2J(H,P_{cis}) = 12 Hz, 1H; RhH) ppm. **$^{31}P\{^1H\}$ NMR** (121.5 MHz, $[D_8]$toluene, 203 K) δ = 13.1 (dt, ^1J(Rh,P) = 93, ^2J(P,P) = 21 Hz, 1P; P *trans* to H), 9.4 (dt, ^1J(Rh,P) = 87, ^2J(P,P) = 22 Hz, 1P), 5.7 (dt, ^1J(Rh,P) = 91, ^2J(P,P) = 22 Hz, 1P) ppm. **^{1}H,^{31}P HMBC NMR** (400.1 MHz/161.9 MHz, $[D_8]$toluene, 203 K) δ = −10.6/13 (d in the ^{1}H domain, ^2J(H,P) = 157 Hz; RhH) ppm.

Formation of $[Rh(GePh_3)(H)(CH_3)(PEt_3)_2]$ (6). (a) A solution of *fac*-$[Rh(GePh_3)(H)(CH_3)(PEt_3)_3]$ (**5**) (65 μmol) in $[D_8]$toluene

(0.5 mL) was generated *in situ* by treatment of $[Rh(CH_3)(PEt_3)_3]$ (**4**) (31 mg, 65 μmol) with $HGePh_3$ (20 mg, 65 μmol) at 203 K and was allowed to warm up to 213 K. The NMR spectroscopic data of the reaction solution revealed after 30 min the intermediate formation of $[Rh(GePh_3)(H)(CH_3)(PEt_3)_2]$ (**6**) along with $[Rh(GePh_3)(PEt_3)_3]$ (**3**), free PEt_3 and unreacted **5** in a ratio 1 : 8 : 1 : 16. Selected NMR data for **6**: **^{1}H NMR** (300.1 MHz, [D$_8$]toluene, 213 K): δ = 0.26 (br s, 3H; CH_3), −11.53 (dt, d in the $^1H\{^{31}P\}$ NMR spectrum ^1J(H,Rh) = 15, $^2J(H,P_{cis})$ = 16 Hz; RhH) ppm. The signals for the ethyl and phenyl groups in **6** are covered by resonances of $[Rh(GePh_3)(PEt_3)_3]$ (**3**) and *fac*-$[Rh(GePh_3)(H)(CH_3)(PEt_3)_3]$ (**5**). **$^{31}P\{^1H\}$ NMR** (121.5 MHz, [D$_8$]toluene, 213 K): δ = 19.3 (d, ^1J(Rh,P) = 115 Hz) ppm. **^{1}H,^{31}P HMBC NMR** (400.1 MHz/161.9 MHz, [D$_8$]toluene, 203 K): δ = −11/19 (s; RhH) ppm.

Synthesis of $[Rh(GePh_3)(CO)_2(PEt_3)_2]$ (7). A slow stream of CO was passed for 1 min through a solution of $[Rh(GePh_3)(PEt_3)_3]$ (**3**) (68 mg, 89 μmol) in benzene (2 mL) at room temperature. The solution turned from dark red to yellow. After stirring for 30 min all volatiles were removed *in vacuo*. The residue was washed once with *n*-hexane (1 mL) and **7** was obtained as a yellow solid. Yield 58 mg (93%). Analytical data for **7**: $C_{32}H_{45}GeO_2P_2Rh$ (701.20): calcd C, 54.97; H, 6.49; found: C, 55.07; H, 6.49. **IR** (ATR) $\tilde{\nu}$ (cm^{-1}): 1964, 1912 (CO). **^{1}H NMR** (300.1 MHz, [D$_6$]benzene): δ = 8.02 (m, 6H; Ph), 7.28 (m, 6H; Ph), 7.20–7.13 (m, 3H; Ph), 1.28 (m, q in the $^1H\{^{31}P\}$ NMR spectrum ^3J(H,H) = 8 Hz, 12H; PCH_2CH_3), 0.81 (dt, ^3J(H,P) = 15, ^3J(H,H) = 8 Hz, 18H; PCH_2CH_3) ppm. **$^{13}C\{^1H\}$ NMR** (75.5 MHz, [D$_8$]thf): δ = 202.4 (dt, ^1J(C,Rh) = 65, ^2J(C,P) = 1 Hz, CO), 148.4 (s; Ph), 136.8 (s; Ph), 128.1 (s; Ph) 128.0 (s; Ph), 21.2 (m, ^1J(C,P) = 11 Hz; PCH_2CH_3), 8.5 (s; PCH_2CH_3) ppm, the assignment of the signals is supported by a ^{1}H,^{13}C HMBC NMR spectrum. **$^{31}P\{^1H\}$ NMR** (121.5 MHz, [D$_6$]benzene): δ = 13.7 (d, ^1J(Rh,P) = 111 Hz) ppm. **MS** (LIFDI, toluene), *m*/*z*: 700 $[M]^+$.

Formation $[Rh(4\text{-}C_5NF_4)(PEt_3)_3]$ (8). 2,3,5,6-Tetrafluoropyridine (2 μL, 0.020 mmol) was added to a solution of $[Rh(GePh_3)(PEt_3)_3]$ (**3**) (15 mg, 0.020 mmol) in [D$_6$]benzene (0.5 mL). After 16 h the quantitative formation of **8** and $HGePh_3$ was observed by NMR spectroscopy. Complex **8** was identified by comparison of its NMR data with the literature.[85]

Formation of $[Rh(C_6F_5)(PEt_3)_3]$ (9). (a) Hexafluorobenzene (0.2 mL) was added to a solution of $[Rh(GePh_3)(PEt_3)_3]$ (18.2 mg, 0.024 mmol) in *n*-hexane (0.2 mL) in a PFA NMR tube. After 5 d at 323 K the quantitative formation of **9** and $FGePh_3$ was observed by NMR spectroscopy. Complex **9** and $FGePh_3$ were identified by comparison of their NMR data with the literature.[91,140]

(b) Pentafluorobenzene (2 μL, 0.018 mmol) was added to a solution of $[Rh(GePh_3)(PEt_3)_3]$ (**3**) (14 mg, 0.018 mmol) in [D$_6$]benzene (0.5 mL). After 36 h the quantitative formation of **9** and $HGePh_3$ was observed by NMR spectroscopy. Complex **9** was identified by comparison of its NMR data with the literature.[91]

Formation $[Rh(4\text{-}C_6F_4CF_3)(PEt_3)_3]$ (10). Octafluorotoluene (3 μL, 0.021 mmol) was added to a solution of $[Rh(GePh_3)(PEt_3)_3]$ (16 mg, 0.021 mmol) in [D$_8$]toluene (0.4 mL) in a PFA NMR tube. After 36 h at 323 K the quantitative formation of **10** and $FGePh_3$ was observed by NMR spectroscopy. Complex **10** and $FGePh_3$ were identified by comparison of their NMR data with the literature.[91,140]

Formation of $[Rh(2\text{-}C_5NF_4)(PEt_3)_3]$ (11) and $[Rh(4\text{-}C_5NF_4)(PEt_3)_3]$ (8). Pentafluoropyridine (2.5 μL, 0.023 mmol) was added to a solution of $[Rh(GePh_3)(PEt_3)_3]$ (**3**) (17.9 mg, 0.023 mmol) in [D$_6$]benzene (0.5 mL). After 23 h the quantitative formation of **11** and **8** in a 10 : 1 ratio as well as the formation of $FGePh_3$ was observed by NMR spectroscopy. Complex **11**, **8** and $FGePh_3$ were identified by comparison of their NMR data with the literature.[56,85,140]

Formation of $[Rh\{(E)\text{-}CF{=}CF(CF_3)\}(PEt_3)_3]$ (12) and $[Rh\{(Z)\text{-}CF{=}CF(CF_3)\}(PEt_3)_3]$ (13). A slow stream of hexafluoropropene was bubbled for 30 s through a solution of $[Rh(GePh_3)(PEt_3)_3]$ (**3**) (30 mg, 0.039 mmol) in *n*-hexane (3 mL) in a PFA tube. After stirring for 8 h at room temperature all volatiles were removed *in vacuo*. The NMR spectroscopic data of the residue reveal the formation of **12** and **13** in a 3 : 1 ratio as well as the formation of $FGePh_3$ and some unidentified fluorine containing species. Complex **13** and $FGePh_3$ were identified by comparison of the NMR data with the literature.[83,140] Selected NMR data for **12**: **^{19}F NMR** (282.4 MHz, [D$_6$]benzene): δ = −64.4 (m, 3F; CF_3), −78.1 (m, 1F; F^α), −148.0 (m, 1F; F^β) ppm. **$^{31}P\{^1H\}$ NMR** (121.5 MHz, [D$_6$]benzene): δ = 18.4 (dddtm, $^1J(Rh,P^b)$ = 120.3, $^2J(P^a,P^b)$ = 39.3, $^3J(P^b,F^\alpha)$ = 24.4, $^4J(P^b,F^\beta)$ = 10.6, 1P; P^b), 11.6 (ddddm, $^1J(Rh,P^a)$ = 145.3, $^2J(P^a,P^b)$ = 39.3, $^3J(P^a,F^\alpha)$ = 6.7, $^4J(P^a,F^\beta)$ = 4.7, $^5J(P^a,F)$ = 0.8, 2P; P^a) ppm. The coupling constants were determined by simulation with gNMR.[88] **^{19}F,^{13}C$\{^1$H$\}$ HMBC NMR** (282.4 MHz/75.4 MHz, [D$_6$]benzene) δ = −64/123 (dm, ^1J(C,F) = 267 Hz; CF_3), −78/190 (dm, ^1J(C,F) = 323 Hz; C^α–F^α), −148.0/140 ppm (dm, ^1J(C,F) = 231 Hz; C^β–F^β).

Synthesis of $[Rh\{(E)\text{-}CF{=}CF(CF_3)\}(\mu\text{-}\kappa^1\text{:}\eta^2\text{-}O_2)(PEt_3)_2]_2$ (14). A slow stream of hexafluoropropene was bubbled for 30 s through a solution of $[Rh(GePh_3)(PEt_3)_3]$ (**3**) (153 mg, 0.17 mmol) in toluene (7 mL) in a PFA tube. After stirring for 12 h at room temperature all volatiles were removed *in vacuo*.

The quantitative formation of $[Rh\{(E)\text{-}CF{=}CF(CF_3)\}(PEt_3)_3]$ (**12**) and $[Rh\{(Z)\text{-}CF{=}CF(CF_3)\}(PEt_3)_3]$ (**13**) in a 6 : 1 ratio as well as the formation of $FGePh_3$ was observed by NMR spectroscopy. The residue was dissolved in benzene (5 ml) and a slow stream of oxygen was bubbled for 30 s through the reaction mixture at 223 K. The solution was allowed to warm up slowly to room temperature. After stirring for 20 min all volatiles were removed *in vacuo*. The residue was washed twice with *n*-hexane (2 mL) and **14** was obtained as a yellow solid after crystallization of a statured toluene/*n*-hexane solution at 243 K. Yield 21 mg (25%). Analytical data for **14**: $C_{30}H_{60}F_{10}O_4P_4Rh_2$ (1004.48): calcd C, 35.87; H, 6.02; found: C, 36.15; H, 5.75. **^{1}H NMR** (300.1 MHz, [D$_6$]benzene): δ = 1.93 (m, 12H; PCH_2CH_3), 1.71 (m, 12H; PCH_2CH_3) 1.01 (m, t in the $^1H\{^{31}P\}$ NMR spectrum ^3J(H,H) = 8 Hz, 36H; PCH_2CH_3) ppm. **^{19}F NMR** (282.4 MHz, [D$_6$]benzene): δ = −65.5 (dd, $^3J(F,F^\beta)$ = 16, $^4J(F,F^\alpha)$ = 8 Hz, 6F; CF_3), −66.5 (dm, $^3J(F^\alpha,P)$ = 29 Hz, 2F; F^α), −143.6 (qm, $^4J(F^\beta,F)$ = 16 Hz, 2F; F^β) ppm. **$^{31}P\{^1H\}$ NMR** (121.5 MHz,

Table 5 Crystallographic data

	2	3	7	14a	14b
Crystal dimensions [mm^3]	0.50 × 0.36 × 0.34	0.40 × 0.35 × 0.30	0.46 × 0.16 × 0.10	0.14 × 0.13 × 0.12	0.31 × 0.07 × 0.01
Crystal color	Yellow	Red	Yellow	Light yellow	Light yellow
Empirical formula	$C_{36}H_{62}GeP_3Rh$	$C_{36}H_{60}GeP_3Rh$	$C_{32}H_{45}GeO_2P_2Rh$	$C_{30}H_{60}F_{10}O_4P_4Rh_2$	$C_{30}H_{60}F_{10}O_4P_4Rh_2$
M	763.26	761.25	699.12	1004.48	1004.48
Crystal system	Monoclinic	Monoclinic	Monoclinic	Monoclinic	Monoclinic
Space group	$P2_1/c$	$P2_1/c$	$P2_1/c$	$P2_1/n$	$P2_1/n$
a [Å]	28.273(5)	11.5439(2)	17.9962(4)	11.5052(14)	10.3168(5)
b [Å]	17.334(3)	22.2499(5)	10.8071(2)	11.7794(12)	18.2065(9)
c [Å]	23.140(4)	18.1297(3)	18.7150(4)	15.3559(17)	11.2497(6)
β [°]	97.339(6)	127.1720(10)	116.882(2)	92.700(5)	95.380(2)
V [Å^3]	11 248.0(4)	3710.51(12)	3246.50(12)	2078.8(4)	2103.75(18)
Z	12	4	4	2	2
$D_{calcd.}$ [mg m^{-3}]	1.352	1.363	1.430	1.605	1.586
μ(Mo-K$_\alpha$) [mm^{-1}]	1.393	1.410	1.559	1.024	1.012
θ range [°]	2.32 to 39.68	2.21 to 28.34	4.58 to 28.40	2.27 to 25.37	1.56 to 25.04
Reflns. collected	498 870	66 019	44 424	18 889	29 343
Indep. reflns.	74 954	9140	7419	3810	3730
R_{int}	0.0876	0.0653	0.0458	0.0331	0.0488
Completeness [%]	99.7	99.7	99.5	99.6	99.5
Absorption correction	Multi-scan	Multi-scan	Multi-scan	Multi-scan	Multi-scan
GoF on F^2	0.996	0.985	1.018	1.008	1.063
R_1, wR_2 on all data	0.1140, 0.0960	0.0298, 0.0464	0.0255, 0.0500	0.0235, 0.0588	0.0334, 0.0549
R_1, w$R_2[I_0 > 2\sigma(I_0)]$	0.0526, 0.0814	0.0214, 0.0449	0.0205, 0.0489	0.0211, 0.0571	0.232, 0.0517
Max. diff. peak/hole [e Å^{-3}]	2.609/−1.255	0.474/−1.083	0.475/−0.912	0.672/−0.577	0.557/−0.488

[D$_6$]benzene): δ = 26.4 (dd, ^1J(Rh,P) = 121, ^3J(P,F) = 29 Hz) ppm. **MS** (LIFDI, toluene), m/z: 1004 [M]$^+$.

Structure determination

Suitable crystals of **2**, **7** and **14a/b** were obtained from saturated toluene/*n*-hexane solutions at 243 K. Dark red crystals of **3** were obtained by slow evaporation of the solvent from a *n*-hexane solution at 243 K. Data collections for **2**, **14a** and **14b** were performed at 100 K with a Bruker D8 Venture area detector and on a STOE IPDS 2θ for **3** and **7**.

The structures were solved by intrinsic phasing (**2**, **14a** and **14b**) and by direct methods (**3** and **7**) (SHELXS-2013) and refined by full matrix least-squares procedures based on F^2 with all measured reflections (SHELXL-2013).[141–143] The SADABS program was used for multi-scan absorption corrections for **2**, **14a** and **14b** and PLATON was used for multi-scan absorption correction of **3** and **7**.[144,145] All non-hydrogen atoms were refined anisotropically. All hydrogen atom positions were placed at their idealized positions and were refined using a riding model except for the rhodium bound hydrogen atoms in **2**, which were found on the electron density map and freely refined. CCDC 1438402 (for **2**), 1438403 (for **3**), 1438404 (for **7**), 1438405 (for **14a**) and 1438406 (for **14b**) contain the crystallographic data (Table 5).

Computational methods

The calculations were run using the Gaussian 09 (Revision D.01) program package[146] and the B3LYP functional. Plausible ligand arrangements for [Rh(GePh$_3$)(H)(CH$_3$)(PEt$_3$)$_2$] were optimized and the structure **6a** turned out to be the minimum. The cc-pVTZ basis sets were employed for all rhodium-bound atoms (cc-pVDZ for all other carbon and hydrogen atoms) except for germanium, which was described on using RECPs with the associated cc-pVTZ-PP basis set.[147] Rhodium was also described on using RECPs with the associated cc-pVTZ-PP basis set.[148] Frequency calculations were run for all stationary points to identify them as minima (no negative eigenvalues). Energies were corrected for zero-point energy.

Acknowledgements

We would like to acknowledge for financial support the DFG research training group "Fluorine as a Key Element" (T. Ahrens) as well as the DFG (BR-2065/8-2). M. Ahrens thanks the "Fonds der Chemischen Industrie". We thank the Solvay Fluor GmbH for a gift of hexafluoropropene. We are grateful to Dipl.-Chem. Cathérine Mitzenheim and Dr. Lada Zámostná for help with the NMR spectroscopy. We would like to thank Silke Hinze for experimental assistance.

References

1 R. E. Banks, *Fluorine Chemistry at the Millennium: Fascinated by Fluorine*, Elsevier, Amsterdam, 2000.
2 T. Hiyama, *Organofluorine Compounds: Chemistry and Applications*, Springer, Berlin, 2000.
3 P. Kirsch, *Modern Fluoroorganic Chemistry: Synthesis, Reactivity and Applications*, Wiley-VCH, Weinheim, 2004.
4 J. A. Gladysz, D. P. Curran and I. T. Horvath, *Handbook of Fluorous Chemistry*, Wiley-VCH, Weinheim, 2006.
5 J. P. Bégué and D. Bonnet-Delpon, *Bioorganic and Medicinal Chemistry of Fluorine*, John Wiley & Sons, Inc., Hoboken, New York, 2008.

6 P. Kirsch, *Modern Fluoroorganic Chemistry: Synthesis, Reactivity, Applications*, Wiley-VCH, Weinheim, 2013.
7 J. L. Kiplinger, T. G. Richmond and C. E. Osterberg, *Chem. Rev.*, 1994, **94**, 373–431.
8 J. Burdeniuc, B. Jedlicka and R. H. Crabtree, *Chem. Ber.*, 1997, **130**, 145–154.
9 T. G. Richmond, *Angew. Chem., Int. Ed.*, 2000, **39**, 3241–3244, (*Angew. Chem.*, 2000, **112**, 3378–3380).
10 T. Braun and R. N. Perutz, *Chem. Commun.*, 2002, 2749–2757.
11 H. Torrens, *Coord. Chem. Rev.*, 2005, **249**, 1957–1985.
12 R. N. Perutz and T. Braun, in *Comprehensive Organometallic Chemistry III*, ed. D. M. P. Mingos and R. H. Crabtree, Elsevier, Oxford, 2007, pp. 725–758.
13 S. A. Macgregor, *Chem. Soc. Rev.*, 2007, **36**, 67–76.
14 R. N. Perutz, *Science*, 2008, **321**, 1168–1169.
15 H. Amii and K. Uneyama, *Chem. Rev.*, 2009, **109**, 2119–2183.
16 G. Meier and T. Braun, *Angew. Chem., Int. Ed.*, 2009, **48**, 1546–1548, (*Angew. Chem.*, 2009, **121**, 1575–1577).
17 R. P. Hughes, *Eur. J. Inorg. Chem.*, 2009, 4591–4606.
18 A. D. Sun and J. A. Love, *Dalton Trans.*, 2010, **39**, 10362–10374.
19 E. Clot, O. Eisenstein, N. Jasim, S. A. Macgregor, J. E. McGrady and R. N. Perutz, *Acc. Chem. Res.*, 2011, **44**, 333–348.
20 T. Braun and F. Wehmeier, *Eur. J. Inorg. Chem.*, 2011, 613–625.
21 A. Nova, R. Mas-Balleste and A. Lledos, *Organometallics*, 2012, **31**, 1245–1256.
22 M. Klahn and U. Rosenthal, *Organometallics*, 2012, **31**, 1235–1244.
23 M. F. Kuehnel, D. Lentz and T. Braun, *Angew. Chem., Int. Ed.*, 2013, **52**, 3328–3348, (*Angew. Chem.*, 2013, **125**, 3412–3433).
24 J. Weaver and S. Senaweera, *Tetrahedron*, 2014, **70**, 7413–7428.
25 T. Ahrens, J. Kohlmann, M. Ahrens and T. Braun, *Chem. Rev.*, 2015, **115**, 931–972.
26 B. L. Edelbach, A. K. F. Rahman, R. J. Lachicotte and W. D. Jones, *Organometallics*, 1999, **18**, 3170–3177.
27 B. M. Kraft, R. J. Lachicotte and W. D. Jones, *J. Am. Chem. Soc.*, 2000, **122**, 8559–8560.
28 B. M. Kraft, R. J. Lachicotte and W. D. Jones, *J. Am. Chem. Soc.*, 2001, **123**, 10973–10979.
29 B. M. Kraft and W. D. Jones, *J. Organomet. Chem.*, 2002, **658**, 132–140.
30 B. M. Kraft and W. D. Jones, *J. Am. Chem. Soc.*, 2002, **124**, 8681–8689.
31 E. Clot, C. Megret, B. M. Kraft, O. Eisenstein and W. D. Jones, *J. Am. Chem. Soc.*, 2004, **126**, 5647–5653.
32 J. Vela, J. M. Smith, Y. Yu, N. A. Ketterer, C. J. Flaschenriem, R. J. Lachicotte and P. L. Holland, *J. Am. Chem. Soc.*, 2005, **127**, 7857–7870.
33 A. A. Peterson and K. McNeill, *Organometallics*, 2006, **25**, 4938–4940.
34 U. Jager-Fiedler, M. Klahn, P. Arndt, W. Baumann, A. Spannenberg, V. V. Burlakov and U. Rosenthal, *J. Mol. Catal. A: Chem.*, 2007, **261**, 184–189.
35 R. D. Rieth, W. W. Brennessel and W. D. Jones, *Eur. J. Inorg. Chem.*, 2007, 2839–2847.
36 S. P. Reade, M. F. Mahon and M. K. Whittlesey, *J. Am. Chem. Soc.*, 2009, **131**, 1847–1861.
37 B. M. Kraft, E. Clot, O. Eisenstein, W. W. Brennessel and W. D. Jones, *J. Fluorine Chem.*, 2010, **131**, 1122–1132.
38 M. F. Kuhnel and D. Lentz, *Angew. Chem., Int. Ed.*, 2010, **49**, 2933–2936, (*Angew. Chem.*, 2010, **122**, 2995–2998).
39 J. A. Panetier, S. A. Macgregor and M. K. Whittlesey, *Angew. Chem., Int. Ed.*, 2011, **50**, 2783–2786, (*Angew. Chem.*, 2011, **123**, 2835–2838).
40 M. F. Kuehnel, P. Holstein, M. Kliche, J. Kruger, S. Matthies, D. Nitsch, J. Schutt, M. Sparenberg and D. Lentz, *Chem. – Eur. J.*, 2012, **18**, 10701–10714.
41 M. F. Kuehnel, T. Schloder, S. Riedel, B. Nieto-Ortega, F. J. Ramirez, J. T. L. Navarrete, J. Casado and D. Lentz, *Angew. Chem., Int. Ed.*, 2012, **51**, 2218–2220, (*Angew. Chem.*, 2012, **124**, 2261–2263).
42 L. Zámostná, M. Ahrens and T. Braun, *J. Fluorine Chem.*, 2013, **155**, 132–142.
43 S. A. Macgregor, D. McKay, J. A. Panetier and M. K. Whittlesey, *Dalton Trans.*, 2013, **42**, 7386–7395.
44 Y. Ishii, N. Chatani, S. Yorimitsu and S. Murai, *Chem. Lett.*, 1998, 157–158.
45 T. Braun, S. P. Foxon, R. N. Perutz and P. H. Walton, *Angew. Chem., Int. Ed.*, 1999, **38**, 3326–3329, (*Angew. Chem.*, 1999, **111**, 3543–3545).
46 M. I. Sladek, T. Braun, B. Neumann and H. G. Stammler, *J. Chem. Soc., Dalton Trans.*, 2002, 297–299.
47 T. Braun, S. Rothfeld, V. Schorlemer, A. Stammler and H. G. Stammler, *Inorg. Chem. Commun.*, 2003, **6**, 752–755.
48 T. Braun, A. Steffen, V. Schorlemer, B. Neumann and H. G. Stammler, *Dalton Trans.*, 2005, 3331–3336.
49 T. Braun, J. Izundu, A. Steffen, B. Neumann and H.-G. Stammler, *Dalton Trans.*, 2006, 5118–5123.
50 T. Braun, V. Schorlemer, B. Neumann and H. G. Stammler, *J. Fluorine Chem.*, 2006, **127**, 367–372.
51 R. J. Lindup, T. B. Marder, R. N. Perutz and A. C. Whitwood, *Chem. Commun.*, 2007, 3664–3666.
52 T. Braun, F. Wehmeier and K. Altenhoener, *Angew. Chem., Int. Ed.*, 2007, **46**, 5321–5324, (*Angew. Chem.*, 2007, **119**, 5415–5418).
53 M. Arisawa, T. Suzuki, T. Ishikawa and M. Yamaguchi, *J. Am. Chem. Soc.*, 2008, **130**, 12214–12215.
54 T. Braun, M. A. Salomon, K. Altenhoner, M. Teltewskoi and S. Hinze, *Angew. Chem., Int. Ed.*, 2009, **48**, 1818–1822, (*Angew. Chem.*, 2009, **121**, 1850–1854).
55 H. L. Buckley, T. Wang, O. Tran and J. A. Love, *Organometallics*, 2009, **28**, 2356–2359.
56 M. Teltewskoi, J. A. Panetier, S. A. Macgregor and T. Braun, *Angew. Chem., Int. Ed.*, 2010, **49**, 3947–3951, (*Angew. Chem.*, 2010, **122**, 4039–4043).

57 L. Keyes, A. D. Sun and J. A. Love, *Eur. J. Org. Chem.*, 2011, 3985–3994.
58 J.-H. Zhan, H. Lv, Y. Yu and J.-L. Zhang, *Adv. Synth. Catal.*, 2012, **354**, 1529–1541.
59 H. Lv, J.-H. Zhan, Y.-B. Cai, Y. Yu, B. Wang and J.-L. Zhang, *J. Am. Chem. Soc.*, 2012, **134**, 16216–16227.
60 L. Sun, M. Rong, D. Kong, Z. Bai, Y. Yuan and Z. Weng, *J. Fluorine Chem.*, 2013, **150**, 117–123.
61 H. Lv, Y.-B. Cai and J.-L. Zhang, *Angew. Chem., Int. Ed.*, 2013, **52**, 3203–3207, (*Angew. Chem.*, 2013, **125**, 3285–3289).
62 T. Ichitsuka, T. Fujita, T. Arita and J. Ichikawa, *Angew. Chem., Int. Ed.*, 2014, **53**, 7564–7568, (*Angew. Chem.*, 2014, **162**, 7694–7698).
63 H. Zhang, J.-H. Lin, J.-C. Xiao and Y.-C. Gu, *Org. Biomol. Chem.*, 2014, **12**, 581–588.
64 A. Singh, J. J. Kubik and J. D. Weaver, *Chem. Sci.*, 2015, **6**, 7206–7212.
65 W.-H. Guo, Q.-Q. Min, J.-W. Gu and X. Zhang, *Angew. Chem., Int. Ed.*, 2015, **54**, 9075–9078, (*Angew. Chem.*, 2015, **127**, 9203–9206).
66 V. V. Grushin, *Chem. – Eur. J.*, 2002, **8**, 1006–1014.
67 C. Bobbio and V. Gouverneur, *Org. Biomol. Chem.*, 2006, **4**, 2065–2075.
68 J. M. Brown and V. Gouverneur, *Angew. Chem., Int. Ed.*, 2009, **48**, 8610–8614, (*Angew. Chem.*, 2009, **121**, 8762–8766).
69 D. A. Watson, M. Su, G. Teverovskiy, Y. Zhang, J. Garcia-Fortanet, T. Kinzel and S. L. Buchwald, *Science*, 2009, **325**, 1661–1664.
70 V. Gouverneur, *Science*, 2009, **325**, 1630–1631.
71 T. Furuya, J. E. M. N. Klein and T. Ritter, *Synthesis*, 2010, 1804–1821.
72 T. W. Lyons and M. S. Sanford, *Chem. Rev.*, 2010, **110**, 1147–1169.
73 T. Furuya, A. S. Kamlet and T. Ritter, *Nature*, 2011, **473**, 470–477.
74 V. Rauniyar, A. D. Lackner, G. L. Hamilton and F. D. Toste, *Science*, 2011, **334**, 1681–1684.
75 C. Hollingworth and V. Gouverneur, *Chem. Commun.*, 2012, **48**, 2929–2942.
76 T. Liang, C. N. Neumann and T. Ritter, *Angew. Chem., Int. Ed.*, 2013, **52**, 8214–8264, (*Angew. Chem.*, 2013, **125**, 8372–8423).
77 M. G. Campbell and T. Ritter, *Chem. Rev.*, 2015, **115**, 612–633.
78 X. Yang, T. Wu, R. J. Phipps and F. D. Toste, *Chem. Rev.*, 2015, **115**, 826–870.
79 Y.-R. Luo, *Comprehensive handbook of chemical bond energies*, CRC Press, 2010.
80 P. P. Samuel, A. P. Singh, S. P. Sarish, J. Matussek, I. Objartel, H. W. Roesky and D. Stalke, *Inorg. Chem.*, 2013, **52**, 1544–1549.
81 M. Aizenberg and D. Milstein, *Science*, 1994, **265**, 359–361.
82 M. Aizenberg and D. Milstein, *J. Am. Chem. Soc.*, 1995, **117**, 8674–8675.
83 T. Braun, D. Noveski, B. Neumann and H. G. Stammler, *Angew. Chem., Int. Ed.*, 2002, **41**, 2745–2748, (*Angew. Chem.*, 2002, **114**, 2870–2873).
84 D. Noveski, T. Braun, M. Schulte, B. Neumann and H. G. Stammler, *Dalton Trans.*, 2003, 4075–4083.
85 D. Noveski, T. Braun, B. Neumann, A. Stammler and H. G. Stammler, *Dalton Trans.*, 2004, 4106–4119.
86 A. Vigalok, L. J. W. Shimon and D. Milstein, *Chem. Commun.*, 1996, 1673–1674.
87 T. Braun, D. Noveski, M. Ahijado and F. Wehmeier, *Dalton Trans.*, 2007, 3820–3825.
88 P. H. M. Budzelaar, *gNMR, Version 4.1*, Adept Scientific plc, Letchworth, 2001.
89 D. L. Thorn and R. L. Harlow, *Inorg. Chem.*, 1990, **29**, 2017–2019.
90 M. Aizenberg, J. Ott, C. J. Elsevier and D. Milstein, *J. Organomet. Chem.*, 1998, **551**, 81–92.
91 A. L. Raza, J. A. Panetier, M. Teltewskoi, S. A. Macgregor and T. Braun, *Organometallics*, 2013, **32**, 3795–3807.
92 M. A. Esteruelas, F. J. Lahoz, E. Onate, L. A. Oro and L. Rodriguez, *Organometallics*, 1996, **15**, 3670–3678.
93 F. Glockling and G. C. Hill, *J. Organomet. Chem.*, 1970, **22**, C48–C50.
94 F. Glockling and G. C. Hill, *J. Chem. Soc. A*, 1971, 2137–2141.
95 K. Osakada, T. Koizumi, S. Sarai and T. Yamamoto, *Organometallics*, 1998, **17**, 1868–1872.
96 K. Osakada, K. Hataya and T. Yamamoto, *J. Chem. Soc., Chem. Commun.*, 1995, 2315–2316.
97 K. Osakada, S. Sarai, T. Koizumi and T. Yamamoto, *Organometallics*, 1997, **16**, 3973–3980.
98 R. D. Adams and E. Trufan, *Inorg. Chem.*, 2010, **49**, 3029–3034.
99 M. Ahijado, T. Braun, D. Noveski, N. Kocher, B. Neumann, D. Stalke and H. G. Stammler, *Angew. Chem., Int. Ed.*, 2005, **44**, 6947–6951, (*Angew. Chem.*, 2005, **117**, 7107–7111).
100 G. Meier and T. Braun, *Angew. Chem., Int. Ed.*, 2011, **50**, 3280–3284, (*Angew. Chem.*, 2011, **123**, 3338–3342).
101 G. Meier and T. Braun, *Angew. Chem., Int. Ed.*, 2012, **51**, 12564–12569, (*Angew. Chem.*, 2012, **124**, 12732–12737).
102 After a multiplication of the FID with a gaussian function the signals at δ = 9.4 and 5.7 ppm resolve to a doublet of doublet of doublets [^{1}J(Rh,P) = 86.7; ^{2}J(P,P) = 21; ^{2}J(P,P) = 24 Hz and ^{1}J(Rh,P) = 91; ^{2}J(P,P) = 21; ^{2}J(P,P) = 23 Hz] in the $^{31}P\{^{1}H\}$ NMR spectrum.
103 A. W. Addison, T. N. Rao, J. Reedijk, J. Vanrijn and G. C. Verschoor, *J. Chem. Soc., Dalton Trans.*, 1984, 1349–1356.
104 S. E. Boyd, L. D. Field, T. W. Hambley and M. G. Partridge, *Organometallics*, 1993, **12**, 1720–1724.
105 A. L. Raza and T. Braun, *Chem. Sci.*, 2015, **6**, 4255–4260.
106 M. I. Sladek, T. Braun, B. Neumann and H. G. Stammler, *New J. Chem.*, 2003, **27**, 313–318.
107 N. A. Jasim, R. N. Perutz, A. C. Whitwood, T. Braun, J. Izundu, B. Neumann, S. Rothfeld and H. G. Stammler, *Organometallics*, 2004, **23**, 6140–6149.

108 S. Burling, P. I. P. Elliott, N. A. Jasim, R. J. Lindup, J. McKenna, R. N. Perutz, S. J. Archibald and A. C. Whitwood, *Dalton Trans.*, 2005, 3686–3695.
109 I. M. Piglosiewicz, S. Kraft, R. Beckhaus, D. Haase and W. Saak, *Eur. J. Inorg. Chem.*, 2005, 938–945.
110 U. Jager-Fiedler, P. Arndt, W. Baumann, A. Spannenberg, V. V. Burlakov and U. Rosenthal, *Eur. J. Inorg. Chem.*, 2005, 2842–2849.
111 T. Schaub, P. Fischer, A. Steffen, T. Braun, U. Radius and A. Mix, *J. Am. Chem. Soc.*, 2008, **130**, 9304–9317.
112 S. Erhardt and S. A. Macgregor, *J. Am. Chem. Soc.*, 2008, **130**, 15490–15498.
113 A. Nova, S. Erhardt, N. A. Jasim, R. N. Perutz, S. A. Macgregor, J. E. McGrady and A. C. Whitwood, *J. Am. Chem. Soc.*, 2008, **130**, 15499–15511.
114 V. V. Grushin, *Acc. Chem. Res.*, 2010, **43**, 160–171.
115 A. Nova, M. Reinhold, R. N. Perutz, S. A. Macgregor and J. E. McGrady, *Organometallics*, 2010, **29**, 1824–1831.
116 E. Jiao, F. Xia and H. Zhu, *Comput. Theor. Chem.*, 2011, **965**, 92–100.
117 S. I. Kalläne, M. Teltewskoi, T. Braun and B. Braun, *Organometallics*, 2015, **34**, 1156–1169.
118 O. Blum, F. Frolow and D. Milstein, *J. Chem. Soc., Chem. Commun.*, 1991, 258–259.
119 M. K. Whittlesey, R. N. Perutz and M. H. Moore, *Chem. Commun.*, 1996, 787–788.
120 B. L. Edelbach and W. D. Jones, *J. Am. Chem. Soc.*, 1997, **119**, 7734–7742.
121 U. von Allwörden and G. V. Röschenthaler, *Chem.-Ztg.*, 1988, **112**, 69–76.
122 A. Penner and T. Braun, *Eur. J. Inorg. Chem.*, 2011, 2579–2587.
123 H. Baumgarth, T. Braun, B. Braun, R. Laubenstein and R. Herrmann, *Eur. J. Inorg. Chem.*, 2015, 3157–3168.
124 J.-C. Choi, K. Kohno, M. Otsuka, H. Yasuda and T. Sakakura, *Organometallics*, 2011, **30**, 6060–6062.
125 T. Kashiwabara, K. Fuse, T. Muramatsu and M. Tanaka, *J. Org. Chem.*, 2009, **74**, 9433–9439.
126 F. A. Cotton, S. J. Kang and S. K. Mandal, *Inorg. Chim. Acta*, 1993, **206**, 29–39.
127 F. A. Cotton, K. R. Dunbar, C. T. Eagle, L. R. Falvello and A. C. Price, *Inorg. Chem.*, 1989, **28**, 1754–1757.
128 Y. Takahashi, M. Hashimoto, S. Hikichi, M. Akita and Y. Moro-oka, *Angew. Chem., Int. Ed.*, 1999, **38**, 3074–3077, (*Angew. Chem.*, 1999, **111**, 3259–3262).
129 M. J. Bennett and P. B. Donaldson, *Inorg. Chem.*, 1977, **16**, 1581–1585.
130 K. Osakada, K. Hataya and T. Yamamoto, *Inorg. Chem.*, 1993, **32**, 2360–2365.
131 X.-Y. Yu, B. O. Patrick and B. R. James, *Organometallics*, 2006, **25**, 4870–4877.
132 M. Paneque, S. Sirol, M. Trujillo, E. Carmona, E. Gutierrez-Puebla, M. A. Monge, C. Ruiz, F. Malbosc, C. Serra-Le Berre, P. Kalck and M. Etienne, *Chem. – Eur. J.*, 2001, **7**, 3868–3879.
133 J. Vicente, J. Gil-Rubio, J. Guerrero-Leal and D. Bautista, *Organometallics*, 2004, **23**, 4871–4881.
134 M. J. Bennett and P. B. Donaldson, *J. Am. Chem. Soc.*, 1971, **93**, 3307–3308.
135 M. J. Bennett and P. B. Donaldson, *Inorg. Chem.*, 1977, **16**, 1585–1589.
136 C. Tejel, M. A. Ciriano, S. Jimenez, V. Passarelli and J. A. Lopez, *Angew. Chem., Int. Ed.*, 2008, **47**, 2093–2096, (*Angew. Chem.*, 2008, **120**, 2123–2126).
137 T. Miyaji, M. Kujime, S. Hikichi, Y. Moro-oka and M. Akita, *Inorg. Chem.*, 2002, **41**, 5286–5295.
138 T. Yoshida, D. L. Thorn, T. Okano, S. Otsuka and J. A. Ibers, *J. Am. Chem. Soc.*, 1980, **102**, 6451–6457.
139 P. J. Zhao and J. F. Hartwig, *Organometallics*, 2008, **27**, 4749–4757.
140 P. D. Prince, G. S. McGrady and J. W. Steed, *New J. Chem.*, 2002, **26**, 457–461.
141 G. M. Sheldrick and T. R. Schneider, *SHELXL: High-resolution refinement*, 1997.
142 G. M. Sheldrick, *SHELXS-2013, Program for Crystal Structure Solution*, University of Göttingen, 2013.
143 G. M. Sheldrick, *SHELXL-2013, Program for Crystal Structure Refinement*, University of Göttingen, 2013.
144 G. M. Sheldrick, *SADABS, Program for Empirical Absorption Correction*, University of Göttingen, 1996.
145 A. L. Spek, *J. Appl. Crystallogr.*, 2003, **36**, 7–13.
146 M. J. Frisch, G. W. Trucks, H. B. Schlegel, G. E. Scuseria, M. A. Robb, J. R. Cheeseman, G. Scalmani, V. Barone, B. Mennucci, G. A. Petersson, H. Nakatsuji, M. Caricato, X. Li, H. P. Hratchian, A. F. Izmaylov, J. Bloino, G. Zheng, J. L. Sonnenberg, M. Hada, M. Ehara, K. Toyota, R. Fukuda, J. Hasegawa, M. Ishida, T. Nakajima, Y. Honda, O. Kitao, H. Nakai, T. Vreven, J. A. Montgomery Jr., J. E. Peralta, F. Ogliaro, M. Bearpark, J. J. Heyd, E. Brothers, K. N. Kudin, V. N. Staroverov, R. Kobayashi, J. Normand, K. Raghavachari, A. Rendell, J. C. Burant, S. S. Iyengar, J. Tomasi, M. Cossi, N. Rega, J. M. Millam, M. Klene, J. E. Knox, J. B. Cross, V. Bakken, C. Adamo, J. Jaramillo, R. Gomperts, R. E. Stratmann, O. Yazyev, A. J. Austin, R. Cammi, C. Pomelli, J. W. Ochterski, R. L. Martin, K. Morokuma, V. G. Zakrzewski, G. A. Voth, P. Salvador, J. J. Dannenberg, S. Dapprich, A. D. Daniels, Ö. Farkas, J. B. Foresman, J. V. Ortiz, J. Cioslowski and D. J. Fox, *Gaussian 09, Revision D.01*, Gaussian, Inc., Wallingford, CT, 2013.
147 K. A. Peterson, *J. Chem. Phys.*, 2003, **119**, 11099–11112.
148 K. A. Peterson, D. Figgen, M. Dolg and H. Stoll, *J. Chem. Phys.*, 2007, **126**, 124101.